Full version of this paper was published at
IEEE Trans Magn. 58 Iss. 2 (Feb. 2022), pp 1-5, DOI 10.1109/TMAG.2021.3085485

A Simplified 2D Equivalent Model for Magnetic Wire Array

Mehran Mirzaei[1], Pavel Ripka[1], and Vaclav Grim[1]

[1]Faculty of Electrical Engineering, Czech Technical University, Prague, 16627, Czech Republic

Demagnetization factor and corresponding apparent permeability for multi-wire arrays using the 3D finite element method are calculated in this paper. The effect of distance between magnetic wires on the demagnetization factor and apparent magnetic permeability is studied for various values of relative magnetic permeability. The simulations are compared with experimental results on arrays up to 91 wires. A novel simplified equivalent 2D model for wire arrays is presented in this paper, as a fast method for calculations. The simplified axisymmetrical model consists of a set of hollow cylinders with equivalent volume. The results of the proposed simplified 2D model fit very well the full 3D FEM simulations and experimental results. Two different hexagonal and square arrangements for wires are considered both for the simulations and the measurements.

***Index Terms*— Apparent permeability, demagnetization, multi wires, 2D and 3D FEM.**

I. Introduction

The calculation of demagnetization factor and apparent permeability of the magnetic core is essential for induction and fluxgate sensors design [1]. Demagnetization factors for ellipsoidal and non-ellipsoidal shapes of a single element were studied in detail in various publications [1]-[13]. For instance, the demagnetization factor for the sphere can be analytically calculated and it is 1/3 [2]. Demagnetization factor for single ellipsoidal has closed-form equation and does not depend on permeability [1]. The apparent permeability is independent of permeability only for very high permeability values. Demagnetization factor for the non-ellipsoidal shape of a single element, for example, solid cylindrical wire and hollow cylinder, cannot be described in single closed-form formula, however, approximations using curve fitting were used [1], [4] and [6]. The magnetic permeability of wire has a high impact on the demagnetization [7]-[8]. The finite element method (FEM) or complex analytical modeling are common methods to take into account magnetic permeability effects on the demagnetization. The demagnetization factors are categorized into two cases: Fluxmetric (ballistic or central) and magnetometric, which considers the whole volume. Magnetometric demagnetization factor is of interest in this paper. In our recent paper [14], we analyzed using 3D FEM the induced voltage of a pickup coil with a core consisting of a wire hexagonal array of up to 91 wires. Magnetic nanowire arrays are fabricated by electroplating into the pores in membranes [15]. These arrays contain millions of wires in every square millimeter. 3D FEM analysis of such complex arrays is not possible due to the computational complexity. We therefore used intuitive simplified 2D model to estimate the demagnetization factor of these arrays.

The aim of this paper is to rigorously define the equivalent 2D model and verify it both by 3D modeling and by experiment on the wires arrays up to 91 wires. We examine the induced voltage in the pickup coils, demagnetization and apparent permeability, for hexagonal and square lattices. Magnetometric demagnetization factor and corresponding apparent permeability are analyzed and calculated using 3D FEM and 2D equivalent model. Various numbers of wires are considered and both linear magnetic permeability and nonlinear *B-H* curve are used for the simulations. The effect of distance between magnetic wires (pitch) on the demagnetization factor and apparent magnetic permeability is studied for various values of relative magnetic permeability.

Using equivalent hollow cylinders instead of wire array would help to simplify the 3D model to a 2D model to simulate: 1- a large number of wires, 2- a model with very fine mesh for higher accuracy, which is problematic in 3D modeling because of limited memory issue.

II. Hollow Cylinder versus Solid Cylinder

Equation (1) depicts the relationship between apparent permeability, μ_a, demagnetization, N and relative magnetic permeability, μ_r.

$$\mu_a = \mu_r/\left(1 + N \cdot (\mu_r - 1)\right), \mu_r \to \infty \Rightarrow \mu_a \approx 1/N$$
$$N = (\mu_r/\mu_a - 1)/(\mu_r - 1) \quad (1)$$

To compare demagnetization and apparent permeability of solid cylinder and hollow cylinder with the same volume, we first used approximate equation of fluxmetric demagnetization factor, N_s according to the formula derived in [4] and [5] for the solid cylinder.

$$N_s(m,\chi) = N_1(m) \cdot 2/\pi \cdot \tan^{-1}(22\chi/m^{1.3}) + N_2(m) \cdot (1 - 2/\pi \cdot \tan^{-1}(22\chi/m^{1.3}))$$
$$\chi = \mu_r - 1, m = L/D \quad (2)$$

$$E(m) = 1/(1-m^2) \cdot \left(1 - m/\sqrt{1-m^2}\cos^{-1}(m)\right), \quad 0 \le m < 1 \quad (3)$$

$$E(m) = 1/(m^2-1) \cdot \left(m/\sqrt{m^2-1}\, ln\left(m + \sqrt{m^2-1}\right) - 1\right), m > 1 \quad (4)$$

Corresponding author: M. Mirzaei (e-mail: mirzameh@fel.cvut.cz).

$$N_1(m) = E(m) \cdot (1 + 2.35\,ln(1 + 0.137m))/(1 + 2.28\,ln(1 + 0.284m)), \quad \mu_r \succ 1 \tag{5}$$

$$N_2(m) = E(m) \cdot 1/(1 + 2.15\,ln(1 + 0.326m)), \mu_r \approx 1 \tag{6}$$

This simplifies for infinite permeability to

$$N_s(m) = 1/m^2 \cdot (ln(1.2m) - 1) \tag{7}$$

where D is the diameter of the wire and L is the axial length of the wire as shown in Fig. 1.

The demagnetization factor N_h of the hollow cylinder with shell thickness h is calculated according to [4]:

$$N_h = (D^2 - (D - 2h)^2)/D^2\, N_s = (1 - (1 - 2h/D)^2)N_s \tag{8}$$

From (8), it is clear that N_h<N_s.

In the following section, we consider 0.2 mm diameter (D) and 36 mm (L) long magnetic wire (m=L/D=180) and calculate the demagnetization factor and apparent permeability of hollow cylinder with the equal cross-sectional area as a solid cylinder or wire.

The magnetic flux distribution in Fig. 1 shows that flux is distributed more smoothly in a hollow cylinder than a solid cylinder because shell thickness is smaller than solid cylinder radius. Fig. 2 shows that the demagnetization factor N_h of the hollow cylinder calculated using (8) is decreasing versus normalized hollow cylinder diameter, D with original solid cylinder diameter, D_s = 0.2 mm and apparent permeability increases with increasing normalized diameter D/D_s (Fig. 2).

III. Wire Array

A. Two wires

Permalloy wires with 36 mm length and diameter 0.2 mm are used for the physical modeling and measurement in this section. Apparent permeability and magnetometric demagnetization factor are calculated based on the averaging formula for volume integral of the axial component of flux density, B_z in wires volume, V_w using (5):

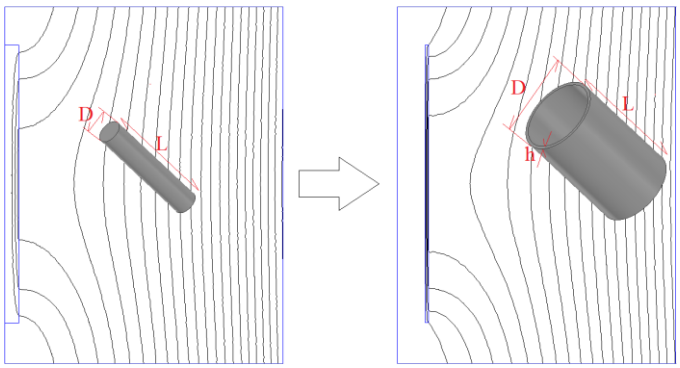

Fig. 1. Magnetic flux distributions in solid cylindrical wire and hollow cylinder or wire with same axial length and volume

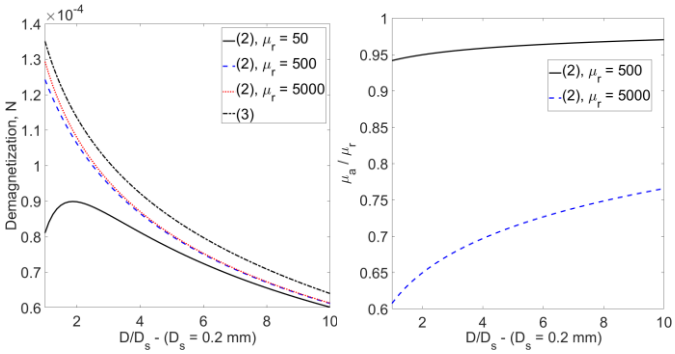

Fig. 2. Demagnetization factor (left) and apparent permeability to relative permeability ratio (right) of the hollow cylinder versus normalized diameter, D/D_s (D_s =0.2 mm) calculated by formulae (2) - (7) - D (mm) is the outer diameter of the hollow cylinder and length L=36 mm (Solid cylinder diameter is 0.2 mm and the hollow cylinder has an equal cross-sectional area as a solid cylinder)

$$\mu_a = \left(\int B_z dV\right)/(B_{air}V_w) \tag{9}$$

Firstly, only two wires are considered to evaluate their magnetostatic coupling. The results are shown in Fig. 3 calculated using magnetostatic 3D FEM, which shows increasing apparent permeability and decreasing demagnetization with increasing the distance of the wires. The magnetostatic coupling is stronger for higher relative magnetic permeability, μ_r = 5000 in comparison with μ_r = 500 and therefore the apparent permeability, $\mu_{a\text{-}2}$ reduces, and demagnetization, N_2 decreases more for the same wire distance.

B. Multi wires

Two possible regular arrangements of wires with equal distances could be hexagonal or square lattices [16]-[17]. It is obvious that for the same wire distance (pitch) the wire density is higher for the hexagonal arrangement in comparison with the square arrangement.

The experimental setup was built to test experimentally the effects of the number of magnetic wires and their distances. Fig. 4 shows a solenoid coil wound around seven wires with the hexagonal arrangement and 5 wires with the square arrangement. The coils with wires are placed in the Helmholtz coils to measure the induced voltage (Fig. 5).

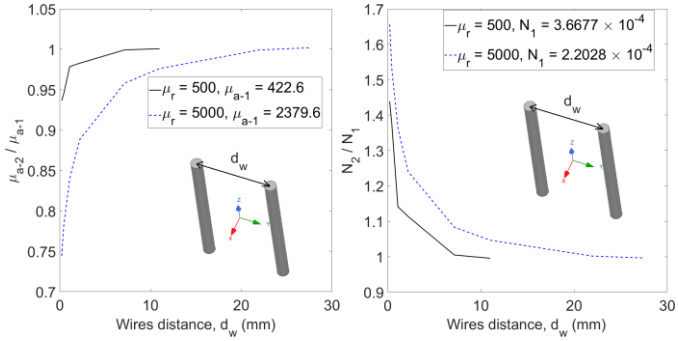

Fig. 3. The ratio of apparent permeability $\mu_{a\text{-}2}$ and demagnetization factor N_2 of two cylindrical wires to those of single wire ($\mu_{a\text{-}1}$ and N_1) as a function of the wire distance

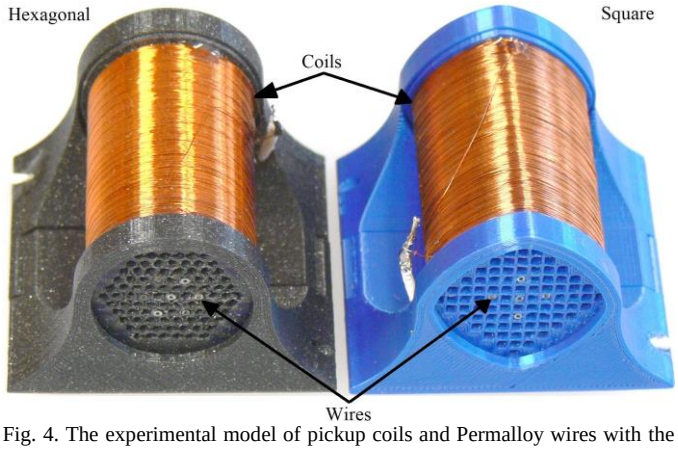

Fig. 4. The experimental model of pickup coils and Permalloy wires with the hexagonal and square arrangement

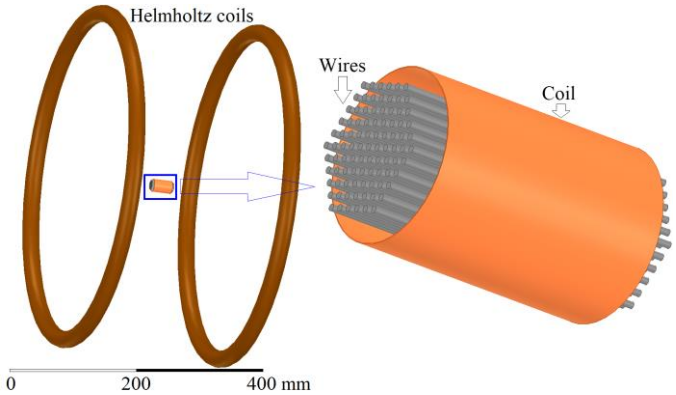

Fig. 5. A computational model of pick up coil and Permalloy wires with the Helmholtz coils to generate a uniform field

Time harmonic method is used for 3D FEM simulations to calculate induced voltages, apparent permeability and demagnetization. The wires and pick up coil are only considered in the model and the Helmholtz coils are substituted by a smooth source field in the air with a value of 34.4 μT - rms as wires and pick coil dimensions are very small in comparison with Helmholtz coils dimensions. The computational model in 3D FEM is reduced to 1/24th of the full model for hexagonal array and 1/16th for a square array to decrease amount of mesh because of axial and circumferential symmetry. The values of induced voltage (normalized by the number of turns of the coil, magnetic flux density generated by Helmholtz coil and frequency) shown in Fig.6 increase with increasing wire distance as apparent permeability of magnetic core increases and demagnetization decreases. The magnetic simulation is shown for μ_r = 17500, which gives the best match between measurements and 3D FEM for both hexagonal and square arrays of wires.

The apparent permeability is higher, and demagnetization is lower for the square array with 5 wires in comparison with the hexagonal array with 7 wires. The lower number of wires causes higher apparent permeability and lower demagnetization. The influence of the increasing distance of wires on demagnetization and apparent permeability is the same as increasing hollow cylinder diameter in Fig. 1 and Fig. 2.

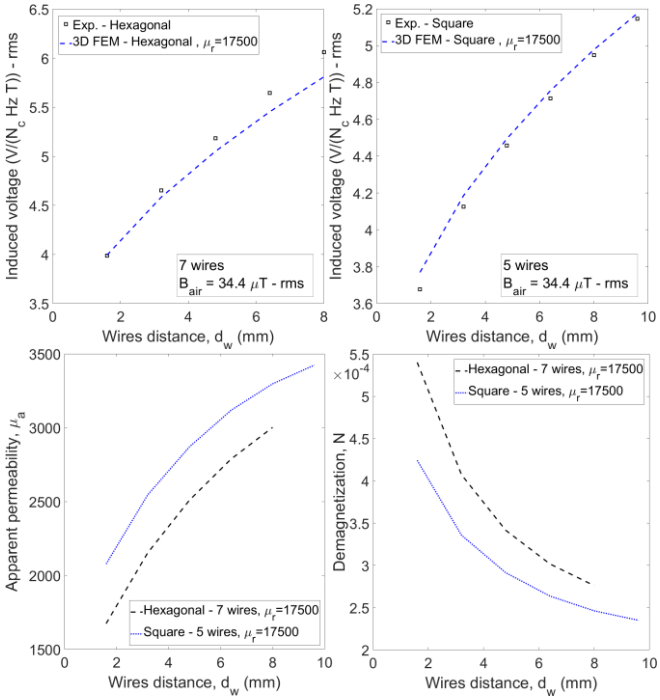

Fig. 6. Normalized induced voltage versus wires distance for hexagonal (7 wires in Fig. 4) and square (5 wires in Fig. 4) array of wires (up) and their apparent permeability and demagnetization (bottom) – 3D FEM with constant permeability

C. 2D Equivalent Model

Regular hexagonal and square distribution of Permalloy wires could be substituted using a hollow cylinder as shown in Fig. 7 to simplify the 3D FEM model to a 2D FEM model with axisymmetric configuration.

The mean radius, R_c of each hollow cylinder is calculated in (10) and (11) so that the corresponding circle area has the same value as areas of the depicted hexagon and square in Fig. 7 for each array of wires. The thickness of the hollow cylinder, t_c in (10) and (11) is calculated with each hollow cylinder volume to be equal to the corresponding array of wires. Practically, all hollow cylinders have the same distance, d_c between each other and the same thickness, t_c because of the regular hexagonal and square distribution of wires.

$$R_c = \sqrt{\frac{3\sqrt{3}}{2\pi}} \cdot R_h,\ d_c = \sqrt{\frac{3\sqrt{3}}{2\pi}} \cdot d_w,\ t_c = \frac{3D_w^2}{4\,d_c} \quad (10)$$

$$R_c = \sqrt{\frac{2}{\pi}} \cdot R_s,\ d_c = \sqrt{\frac{2}{\pi}} \cdot d_w,\ t_c = \frac{D_w^2}{2\,d_c} \quad (11)$$

where, d_w and D_w are wires distance and diameter of wires, respectively.

Fig. 8 presents 2D magnetic flux distribution for a hexagonal array of wires with 91 wires and a square array of wires with 85 wires using 2D axisymmetric time harmonic FEM.

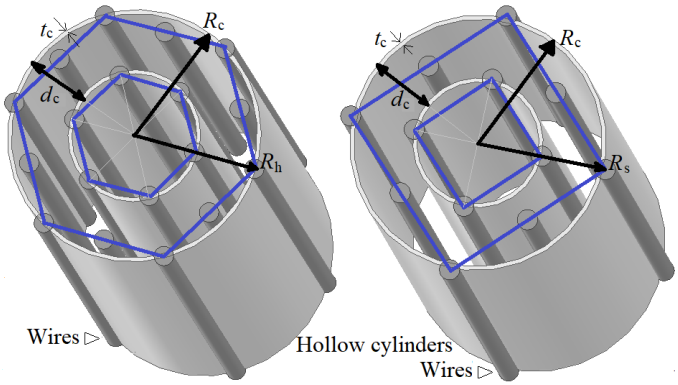

Fig. 7. The schematic model of wires for hexagonal array (left) and square array (right) and their equivalent hollow cylinder model for 2D analysis

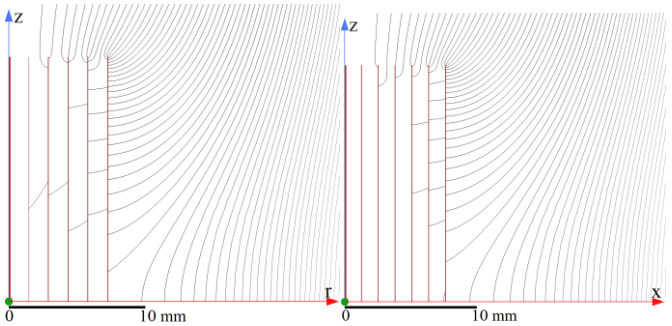

Fig. 8. Magnetic flux distribution in a 2D axisymmetric model of hexagonal distributions of 91 wires with 5 arrays (left) and square distribution of 85 wires with 6 arrays (right)

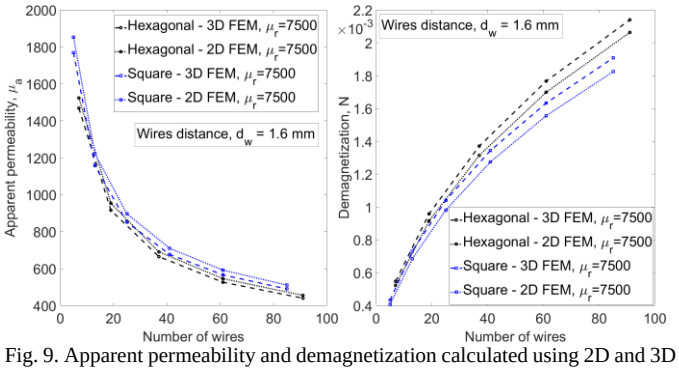

Fig. 9. Apparent permeability and demagnetization calculated using 2D and 3D FEM versus number of wires with hexagonal and square distribution – Constant permeability

The calculated hollow cylinders corresponding to the square array of wires have a 1.28 mm distance and 15.7 µm thickness, and they are 1.46 mm and 20.6 µm for a hexagonal array of wires. The comparisons between 3D FEM and 2D axisymmetric FEM for apparent permeability and demagnetization versus the number of wires are shown in Fig. 9. The small discrepancy is mainly caused by less fine mesh in 3D mode in comparison with 2D model.

IV. Induced Voltage

The calculated induced voltage using the 2D equivalent model versus the number of wires with wires distance 1.6 mm are investigated. The linear magnetic permeability and nonlinear *B-H* curve are both considered for the modeling to evaluate the accuracy of the 2D equivalent model based on hollow cylinders for the multi wire arrays.

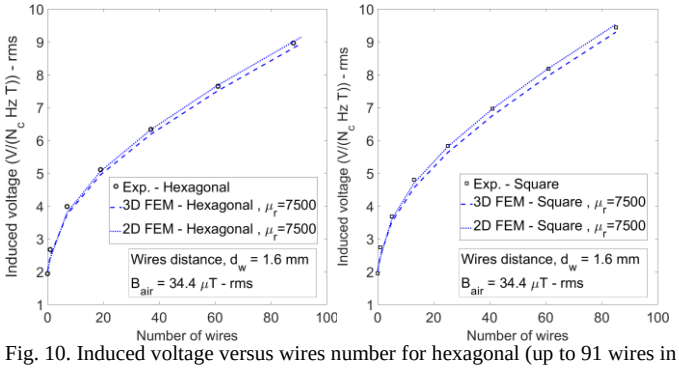

Fig. 10. Induced voltage versus wires number for hexagonal (up to 91 wires in Fig. 5) and square (up to 85 wires) array of wires- 3D FEM and 2D FEM with constant permeability versus experimental results

A. Linear Simulations and Constant Permeability

Fig. 10 shows normalized induced voltage versus the number of wires, comparing experimental results, 3D FEM and 2D FEM using equivalent model under homogenous magnetic field in the air with B_{air} = 34.4 μT - rms. The 2D FEM matches with 3D FEM and experiments with higher accuracy for induced voltage in comparison with results in Fig. 9. The reason is that the induced voltage in the pickup coil is less sensitive to the mesh quality.

B. Nonlinear B-H curve

A typical *B-H* curve for Permalloy material of measured wires in this paper is utilized to model nonlinearity [18]. The following analytical formulas [19] in (12) and (13) are used in FEM simulations for smooth modeling of the *B-H* curve. Using analytical functions in (12) and (13) helps to generate a *B-H* data for smooth magnetization curve, which is essential for accurate FEM analysis of Permalloy wires.

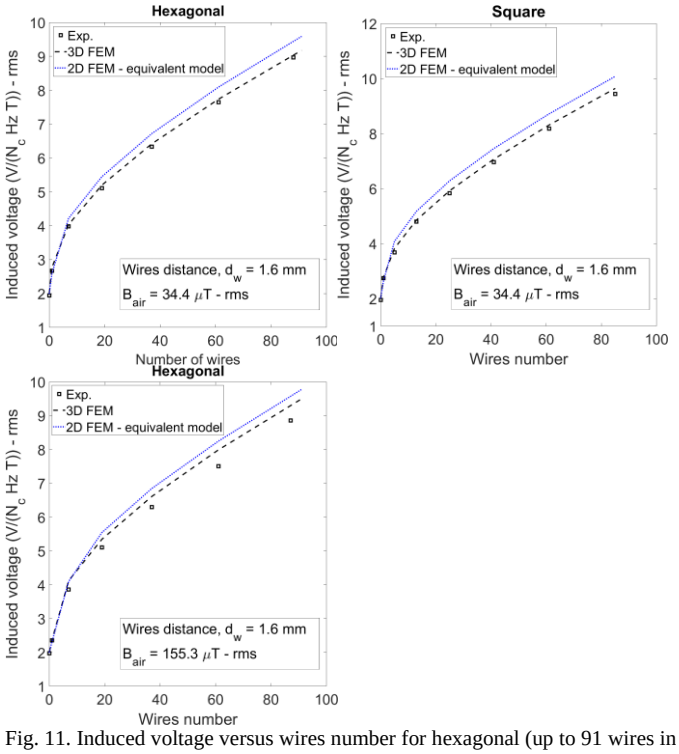

Fig. 11. Induced voltage versus wires number for hexagonal (up to 91 wires in Fig. 5) and square (up to 85 wires) array of wires- 3D FEM and 2D FEM with nonlinear *B-H* curve versus experimental results

$$B = J + \mu_0 H, \qquad \mu_r = \frac{1}{\mu_0}\frac{B}{H} = \frac{1}{\mu_0}\frac{J}{H} + 1$$

(12)

$$\mu_r = \frac{1}{\mu_0}\frac{a_1 H^{b_1-1} + a_2 H^{b_2-1}}{c_1 H^{b_1} + c_2 H^{b_2} + 1} + 1$$

(13)

The parameters a_1, a_2, c_1, c_2, b_1 and b_2 in (13) are $14.1 \cdot 10^{-3}$, $3.11 \cdot 10^{-3}$, $43.2 \cdot 10^{-3}$, $5.48 \cdot 10^{-3}$, 2.17 and 3.78, respectively. The results of the induced voltage at applied fields 34.4 μT and 155.3 μT are shown in Fig. 11. The discrepancy is higher between 3D FEM and 2D FEM for nonlinear simulations in comparison with the linear simulations in Fig. 10. However, the accuracy of the equivalent 2D model is in an adequate range in comparison with experimental results. Utilizing a 2D equivalent model could help to decrease simulation time especially when a nonlinear *B-H* curve should be used for example for fluxgate sensors analysis, design, and optimization.

V. Conclusion

Apparent permeability and magnetometric demagnetization factors of cylindrical wire arrays were analyzed and calculated. The distance between wires is a critical factor for apparent permeability and demagnetization. Two different wire lattices are considered: hexagonal and square. The difference of apparent permeability and demagnetization factor for hexagonal and square arrangements of wires decreases when wires distance decreases as magnetostatic coupling between wires becomes higher and multiwire perform as a single solid wire. Increasing wire distance increases apparent permeability and decreases the demagnetization factor, which is similar to the comparison between the solid cylinder and hollow cylinder.

The novel 2D equivalent model based on hollow cylinders to replace the 3D model was proposed and verified by measurement. 2D model could save the time of simulations and number of cells in the mesh and speed up design and optimization of magnetic sensors with multiwire core.

Acknowledgment

This study was supported by the Grant Agency of the Czech Republic within the Nanofluxgate project (GACR GA20-27150S).

References

[1] P. Ripka, *Magnetic Sensors and Magnetometers*, Artech House Publishers, Jan. 2001

[2] M. Stafl, *Electrodynamics of Electrical Machines*, Publisher: Iliffe , 1st March 1968

[3] S. G. Sandomirskii, "Calculation of short hollow cylinders under magnetization parallel to the generatrix," *Russian Electrical Engineering*, vol. 80, pp. 109–112, Feb. 2009

[4] S. G. Sandomirskii, "Errors in the classical calculation of the demagnetizing factor for a cylinder," *Russian Electrical Engineering*, vol. 84, pp. 376-381, Feb. 2013

[5] V. F. Matyuk, A. A. Osipov, and A. V. Strelyukhin, "Central demagnetization coefficient for hollow cylindrical bars made of soft magnetic materials," *Russian Journal of Nondestructive Testing*, vol. 43, no. 3, pp. 154–162, 2007

[6] M. Nirei, S. Suzuki, K. Tashiro, and H. Wakiwaka, "Constitution of an approximate equation of demagnetizing factors for cylinder using multiple regression analysis", *Journal of the Japan Society of Applied Electromagnetics and Mechanics*, vol. 17, no. 3, pp. 449-452, 2009

[7] D.-X. Chen, J. A. Brug, and R. B. Goldfarb, "Demagnetizing factors for cylinders", IEEE Trans. On Magnetics, vol. 27, no. 4, pp. 3601-3619, 1991

[8] D.-X. Chen, E. Pardo, A. Sanchez, "Fluxmetric and magnetometric demagnetizing factors for cylinders," *Journal of Magnetism and Magnetic Materials*, vol. 306, pp. 135–146, 2006

[9] M. Beleggia, D. Vokoun, M. DeGraef, "Demagnetization factors for cylindrical shells and related shapes," *Journal of Magnetism and Magnetic Materials*, vol. 321, pp. 1306–1315, 2009

[10] J. Prat-Camps, C. Navau, D.-X. Chen, and A. Sanchez, "Exact analytical demagnetizing factors for long hollow cylinders in transverse field," *IEEE Magnetics Letters*, vol. 3, 0500104, 2012

[11] B. K. Pugh, D. P. Kramer, and C. H. Chen, "Demagnetizing factors for various geometries precisely determined using 3-D electromagnetic field simulation," *IEEE Trans. on Magnetics*, vol.47, no.10, pp. 4100-4104, Oct. 2011

[12] S. H. Im and G. S. Park, "Research on the demagnetization and demagnetizing factors for normal shape of magnetic materials," *Compumag* 2017, 18-22 June, Daejeon, Korea, 2017

[13] S. H. Im, and G. S. Park, "A research on the demagnetizing factors for magnetic hollow cylinders," 2018 21st *International Conference on Electrical Machines and Systems* (ICEMS) October 7-10, Jeju, Korea, 2018

[14] P. Ripka, V. Grim, M. Mirzaei, "The apparent permeability and the amplification factor of magnetic wires and wire arrays,' *J. of Magnetism and Magnetic Materials*, vol. 527, no. 1, 167726, June 2021.

[15] P. Ripka, V. Grim, M. Mirzaei, D. Hrakova, J. Uhrig, F. Emmerich, C. Thielemann, J. Hejtmanek, O. Kaman and R. Tesar, "Modeling and measurement of magnetically soft nanowire arrays for sensor applications," *Sensors*, vol. 21, no. 1, 3, 2021

[16] A. A. Woodworth, Ralph Jansen, K. Duffy, P. Naghipour, and E.-S. Shin, "Creating a multifunctional composite stator slot material system to enable high power density electric machines for electrified aircraft applications," 2018 AIAA/IEEE Electric Aircraft Technologies Symposium, pp. 1-8, July 9-11, 2018, Cincinnati, Ohio

[17] P. A. Kyaw, M. Delhommais, J. Qiu, C. R. Sullivan, J.-L. Schanen, and C. Rigaud, "Thermal modeling of inductor and transformer windings including litz wire," *IEEE Trans. on Power Electronics*, vol. 35, no. 1, pp. 867-881, Jan. 2020

[18] J. Kubik, L. Pavel, P. Ripka, P. Kaspar, "Low-power printed circuit board fluxgate sensor," *IEEE SENS. J.*, vol. 7, no. 2, pp. 179-183, 2007

[19] M. Mirzaei M, P. Ripka, "Analytical functions of magnetization curves for high magnetic permeability materials," *IEEE Trans. Magn.*, vol. 54, 2002105, 2018